Chapter 8. High Speed Machining

High Performance Machining for Die/Mold Manufacturing – R&D in Progress

Keynote Paper

Taylan Altan (altan.1@osu.edu)
The Ohio State University, Columbus, Ohio, USA

Mahmoud Shatla, Yung-Chang Yen and Nuri Akgerman
The Ohio State University, Columbus, Ohio, USA

Key words: high-speed machining, PCBN inserts, die/mold manufacturing, FEM, flow stress, roughing, finishing, sculptured-surface machining, OPTIMILL, analytical modeling of machining, OXCUT

Abstract: This paper presents current progress in high performance machining research on die and mold manufacturing. This work is being conducted at the Engineering Research Center for Net Shape Forming (ERC/NSM) for a number of manufacturing companies and covers: a) theoretical and experimental studies of tool failure and tool life in high speed milling of hard materials, b) optimization of CNC programs by adjusting spindle RPM and feed rate (program OPTIMILL) to maintain nearly constant chip load in machining sculptured surfaces, and c) prediction of chip flow, stresses and temperatures in the cutting tool as well as residual stresses in the machined surface layer. Experimental studies are conducted using a 4-axis HMC with 14,000 rpm spindle and 40 m/min feed rate. Tool materials evaluated for tool life and failure include carbides, coated carbides, and PCBN. Workpiece materials investigated include H13 at 46 HRC, P20 at 20 to 40 HRC, and cast iron. Predictions of temperatures and stresses are made using the expanded capabilities of a commercially available FEM code, developed for the analysis of large plastic deformations.

1. INTRODUCTION

1.1 Basics of Die/Mold Manufacturing

Dies and molds are composed of functional and support components. In injection molding and die casting, the functional components are cavities and core inserts, or called die cavities in forging. In stamping, they are often referred to as punch and die. Cavities and core inserts are usually machined out of solid blocks of die steel. However, large stamping dies and punches are often cast to near-final geometry with a machining allowance added. By using standard support components, which assure the overall functionality of tooling assembly, the time necessary for manufacturing a die/mold is reduced, and machining is mainly devoted to producing the core and cavity, or the punch and die.

The information flow and processing steps used in traditional die/mold manufacturing may be divided into die/mold design (including geometry transfer and modification), tool path generation, rough machining (of die block and/or EDM electrode), finish machining (including semi-finishing where necessary), manual finishing or benching (including manual and automated polishing), and tryout. An information flow model is presented in Figure 1.

In the manufacturing of dies and molds, a great portion of the lead time is spent for machining and polishing operations, as outline for stamping in Fig. 2. Though surface finish is not as critical as for injection molds, dies for sheet metal forming still take up to 40% of the processing time for machining but around 20% for polishing/manual finishing. The numbers for injection molds and die casting dies lie between these figures. Surface finish requirements for injection molds are higher than forging and stamping dies, but complex geometry impedes

The original version of this chapter was revised: The copyright line was incorrect. This has been corrected. The Erratum to this chapter is available at DOI: 10.1007/978-0-387-35392-0_40

G. J. Olling et al. (eds.), *Machining Impossible Shapes*

the application of automated polishing. Therefore, it is not surprising that the machining and polishing portion of a die/mold manufacturing job represents two third of the total manufacturing costs [1]. Attempts to increase productivity and reduce costs should start with the efforts to reduce the lead time involved in machining and polishing processes.

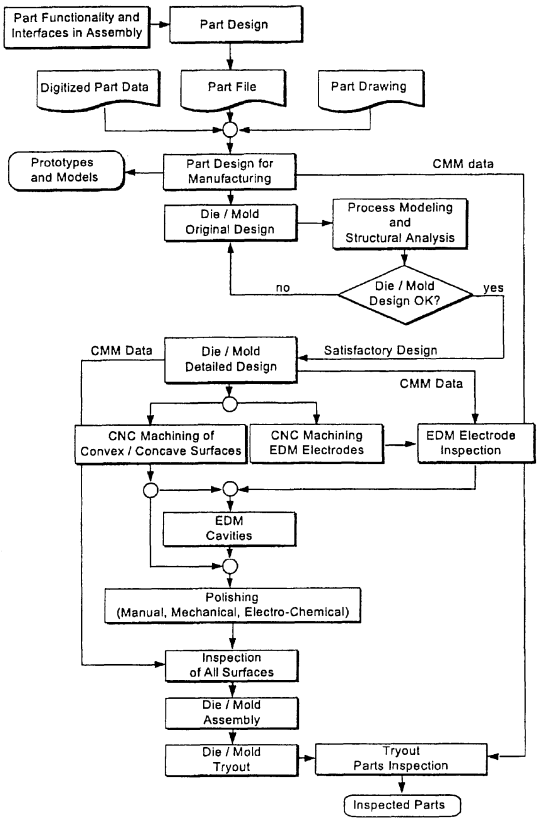

Figure 1. Information flow and processing steps in die / mold manufacturing

1.2 High Performance Machining

With the advances in machine tools and cutting tool materials, High-speed Milling/Machining (HSM) has become a cost-effective manufacturing process to produce parts with high precision and surface quality. Recently, HSM is applied to machining of alloy steels (usually hardness > 30 HRC) for making dies/molds used in production of automotive and electronic parts, as well as plastic molding parts [1]. The definition of HSM is based on the type of workpiece material being machined. Figure 3 shows generally accepted cutting speeds in high-speed machining of various materials [2]. For instance, a cutting speed of 500 m/min is considered high-speed machining for alloy steel, whereas this speed is considered conventional in cutting aluminum. Major advantages of high-speed machining are reported as high material removal rates, reduction in lead times, low cutting forces, decrease in workpiece distortion, and improvement of part precision and surface finish. However, the problems associated with HSM application differ with the work material and desired part geometry. The common disadvantages of high-speed machining are claimed to be excessive tool wear,

the need for expensive machine tools with advanced spindles and controllers, fixturing, balancing of the tool holder, and most importantly, the need for advanced tool materials and coatings.

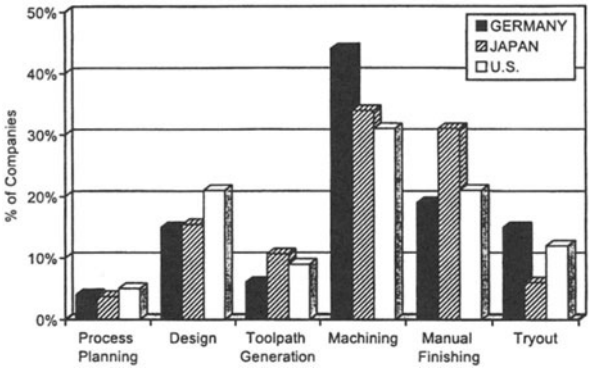

Figure 2. Lead time for each step in stamping die manufacturing

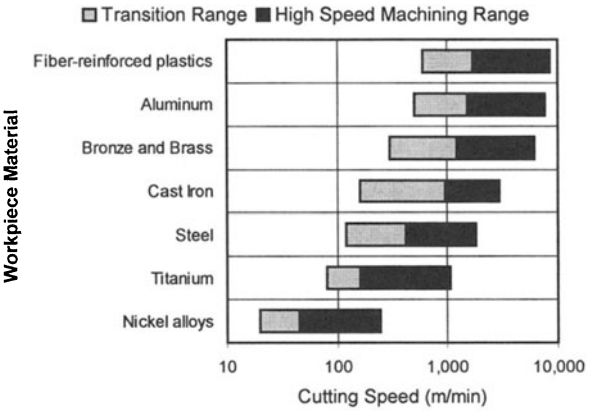

Figure 3. Cutting speed ranges in machining of various material [2]

Parallel to the increase in HSM applications, there is an increase in research for the development of new cutting tool materials, design of cutting tool inserts, new strategies for CNC cutter path generation, and optimization for cutting conditions. Furthermore, computer-aided simulation of cutting processes are emerging as useful techniques for predicting tool temperatures and stresses and for evaluating tool life.

2. APPLICATIONS OF HIGH-SPEED MILLING

High-speed milling of aluminum alloys has been practiced extensively in aerospace industry for more than one decade. Recent applications of HSM are mainly in hard turning, die/mold manufacturing, and machining of castings. The goal of the high-speed milling research was to determine the performance of advanced cutters and identify recommended cutting speeds and feed rates. At the ERC/NSM, the investigation was focused on machining time and surface finish. For these purposes, the milling experiments were performed on a 4-axis high-speed horizontal milling center (Fig. 4). Indexable ball end milling inserts were

used and one of the two cutting edges was ground to avoid the influence of tool run-out on tool wear.

Three work materials, including cast iron, P20 (30 HRC), and H13 (46 HRC), were investigated for HSM applications at ERC/NSM. The alloyed cast iron with the GM specification GM241 (at hardness of 210 HBN) is primarily utilized for manufacturing stamping dies. P20 mold steel is by far the most common steel for injection molds. Due to its low carbon content, it is usually machined in its pre-hardened state (30 HRC) and is subsequently case hardened to 50~55 HRC. In the applications for die casting dies, the hot work die steel H13 is finish machined at 46 HRC.

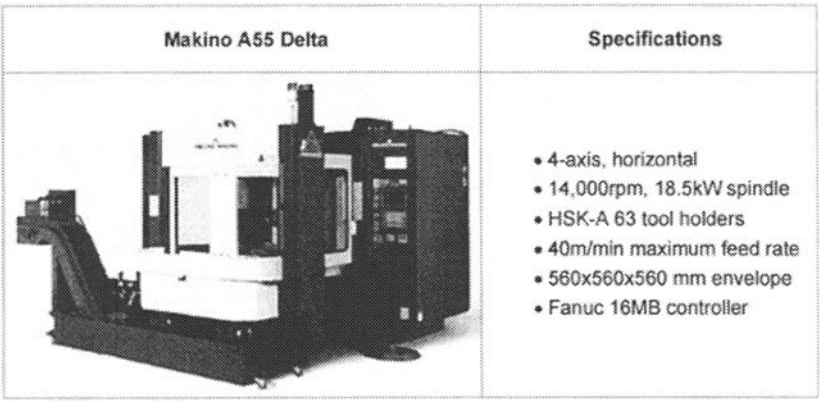

Figure 4. High-speed milling center used in present research

The cutting performances for various tool materials (PCBN, uncoated, TiN, TiCN, and TiAlN coated carbide inserts) were compared through experiment. The tool geometry and cutter specifications are given in Fig. 5. PCBN 2 with 90% CBN and a metallic binder phase was selected for all three workpiece materials. Tests for cast iron were also performed with PCBN 0, which contains 65% CBN and a ceramic binder phase based on titanium nitride (TiN). The PCBN inserts consisted of an approximately 0.8 mm thick layer of PCBN brazed on a carbide base. Besides, the cutting edge of the PCBN inserts was prepared with a hone of 25μm.

2.1 High Speed Milling of Cast Iron

In machining of cast iron, coated carbides, CBN, and SiN tools are most commonly used. In the present study, coated carbides and selected CBN grades were investigated. Using TiN-coated carbide inserts instead of uncoated tools increases productivity in terms of cutting speed by 25% while tool life increases by more than 500%. In addition, TiAlN-coated inserts cut at least three times longer than TiN- or TiCN-coated inserts at any cutting speed, Fig. 6. However, PCBN inserts outperformed the coated carbide inserts. Tool life tests were aborted after surface area of 1.6 m^2 was machined. Tool wear on PCBN 2 was measured at VB_{max} = 60 μm and at VB_{max} = 85 μm on PCBN 0. Abrasion and thermal fatigue were identified as the main wear mechanisms. Higher CBN content and higher hardness exhibited favorable wear resistance.

To investigate the influence of cutting speed on surface finish, CBN tools were operated at a feed rate of 0.5 mm/tooth and cutting speeds varied from 2.8 to 750 m/min. At comparably low cutting speeds from 2.8 to 10 m/min, the surface finish quality was unacceptable due to the formation of built-up edge. Surface roughness decreased with an increasing cutting speed. Once the cutting speed exceeded 300 m/min, this effect tapered off. R_Z=8.3 μm was measured at the maximum cutting speed of V_C=750 m/min (see Fig. 7). Similar results were obtained for various coatings (TiN, TiCN, TiAlN) and CBN.

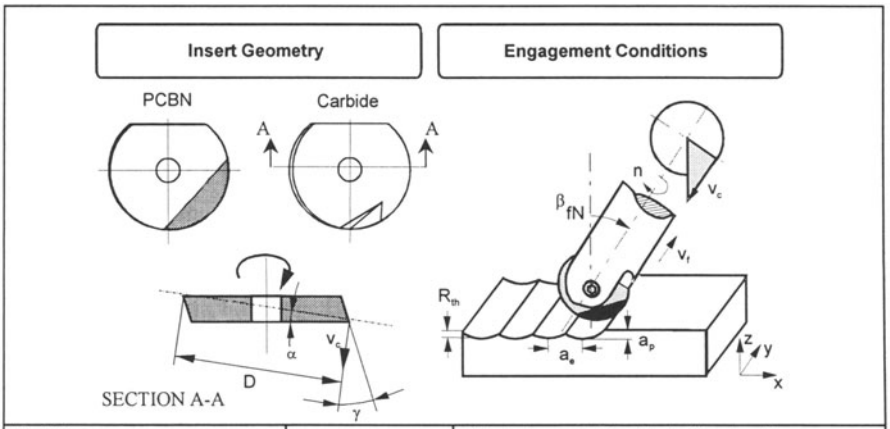

Tool Type		Single insert indexable ball end mill
Tool Diameter	D [mm]	25.4
No. of Cutting Edges	Z	1
Tool Geometry	[°]	$\alpha = 16, \gamma = -9$
Tilt Angle	β_{fN} [°]	30
Lead Angle	β_f [°]	0
Tool Life Criterion	VB [mm]	0.150

Figure 5. Tool geometry and tool life criterion used for the cutting tools

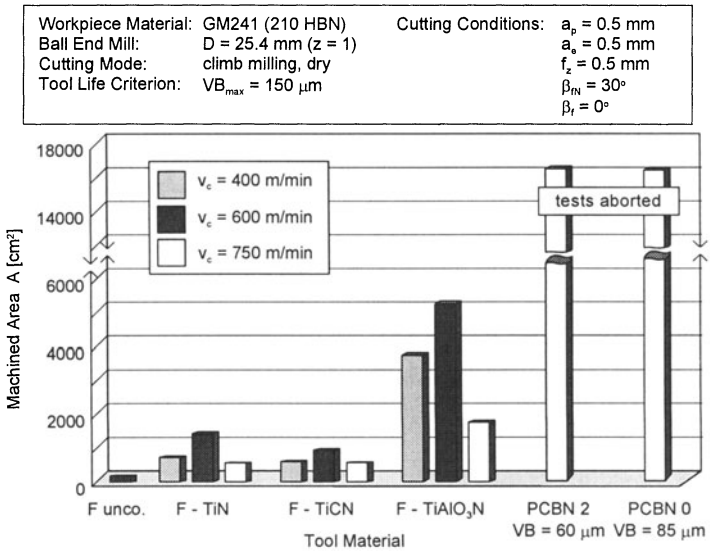

Figure 6. Summary of all tool life experiments in pearlitic cast iron

Based on the studies conducted at ERC/NSM and experiences obtained in various die shops, the application of CBN cutting tools on finishing of gray cast iron is highly recommended because of their superior performance in terms of tool life and surface finish. Harder grades of PCBN with metallic binder phases and high CBN content such as PCBN 2

are expected to perform better than PCBN materials with ceramic binder phases and lower CBN content. The difference in tool life and surface finish between conventional milling and climb milling can be neglected.

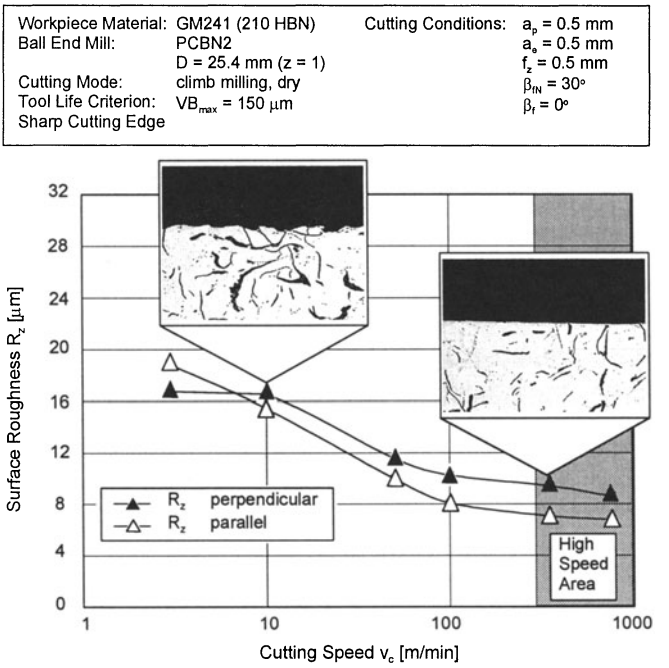

Figure 7. Influence of cutting speed on surface finish when cutting cast iron

2.2 High Speed Milling of P20

In machining of P20 mold steel, the performance of uncoated carbide inserts was inferior to the other tool materials even at the lowest cutting speed of V_C= 300 m/min due to accelerated flank and crater wear (Fig. 8). It can be assumed that the temperatures on the cutting edge already exceeded T = 700°C, which is the oxidation barrier for carbide tooling. TiN-coated carbide tools performed better than TiAlN- and TiCN-coated inserts. PCBN 2 exhibited less flank wear than TiN-coated tools, but failed due to chipping after the area A= 0.56 m^2 was finish machined.

The tests at V_C = 550 m/min showed that tool wear on coated inserts developed at similar rates. Even at these conditions, TiAlN and TiCN coatings did not outperform TiN coating. Wear in PCBN 2 was developing at a very slow rate, and the test was aborted after A = 1.27 m^2. At this stage, the flank wear on this insert was measured to be VB = 82 µm. The PCBN 2 insert at V_C= 800 m/min wore out after A= 0.375 m^2 was machined. Nevertheless, when comparing the results for V_C= 550 and 800 m/min, it was found that for approximately the same tool life, productivity can be increased by 30% when using PCBN 2 instead of coated carbides.

As in the machining of cast iron, PCBN 2 inserts also yielded the best surface finish when cutting P20, Fig. 9. The roughness measurements were taken after the inserts reached the end of tool life at VB=150 µm with the exception of PCBN 2 for V_C=550 m/min. With PCBN inserts, surface roughness R_Z of less than 5 µm could be achieved at 550 m/min as well as at 800 m/min. Despite the comparably low hardness of the workpiece, the use of PCBN 2 cutting tools can be recommended for finish machining of P20. However, it has to be

considered that the conditions prevailing at cutting speeds around V_C=300 m/min lead to insert fracture.

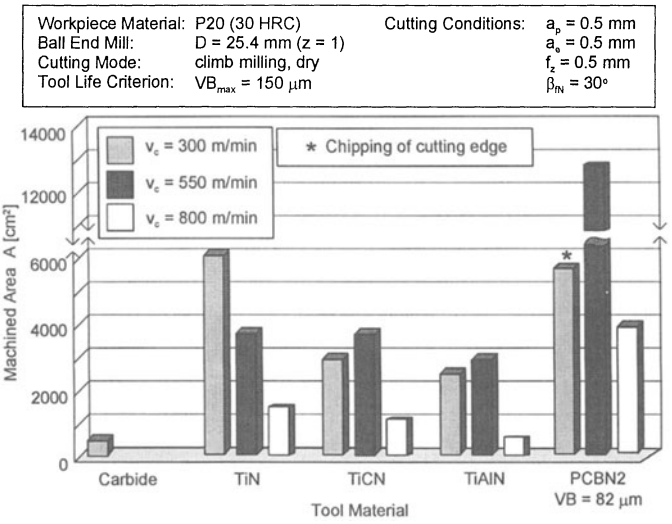

Figure 8. Performance of different tool materials in HSM of P20

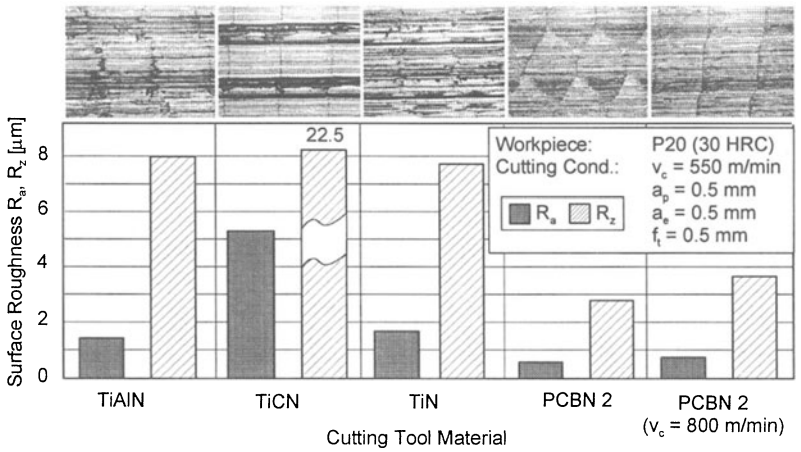

Figure 9. Surface finish with different cutting materials in HSM of P20

2.3 High Speed Milling of H13

In machining of H13 die steel, TiN-coated carbide inserts outperformed the other coated carbide and PCBN 2 inserts at the cutting speeds V_C= 300 and 450 m/min, Fig. 10. For PCBN inserts, the longest tool life in terms of finished area was achieved at a cutting speed of V_C= 800 m/min (A= 1875 cm^2). At these conditions, TiN-coated inserts reached the end of tool life criterion after an area of 750 cm^2 was finished. Compared to stamping dies and injection molds, die casting dies and forging dies consist of fairly intricate geometries. If the chip thickness was maintained, a cutting speed of 800 m/min would require a feed rate of 6.9 m/min. Considering the acceleration and deceleration capabilities of machining centers

available on the market today, it is impossible to achieve on fairly small die geometry. Consequently, PCBN 2 inserts should not be considered and TiN coated carbide inserts are recommended for the finishing of H13 dies. The optimum cutting speed was found to be V_C = 450 m/min.

3. OPTIMIZATION OF CNC PROGRAM IN MILLING SCULPUTRED SURFACES

3.1 High Performance Machining – Roughing

In roughing operations, whenever possible it is desirable to enter the workpiece from the top. The preferred method is to use a helical motion as shown in Fig. 11. The helical motion should maintain a constant diameter and downward velocity. In order not to have any material left on the top, the diameter of the helical motion should be sufficiently less than two times the diameter of the tool. It is very important to remember that the plunging capability of some tools is limited. When a cutter approaches a corner, chip thickness and engagement angle increase dramatically, causing a thermal and mechanical shock in the tool, Fig. 12. This can be significantly reduced by placing a small arc in the tool path. This condition improves with an increasing arc angle, but with the aftereffect of an increase of material left in the corner. The corner material can then be removed using a smaller tool.

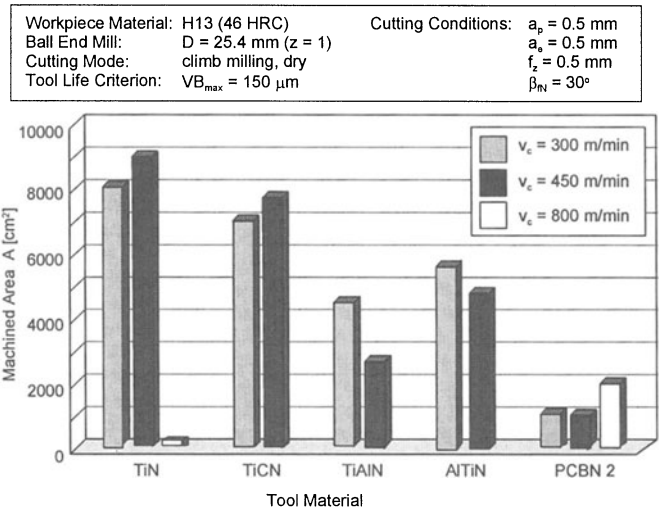

Figure 10. Performance of different cutting materials in HSM of H13

3.2 High Performance Machining – Finishing

The main purpose of high-speed milling is to diminish the effort for manual polishing and, at the same time, get the finishing job done as quickly as possible. Improved surface finishes are achieved through an increased number of finishing paths. The step over distance or pick feed in combination with tool radius determines the theoretical surface roughness. Since the maximum cutter radius is limited by part geometry, especially fillet radii, the only way to minimize the theoretical surface roughness is to minimize the step over distance, which results in an increase in machining time. To compensate this increasing time effort, higher feed rates and spindle speeds, which result in higher surface cutting speeds, have to be applied. Higher temperatures and accelerated tool wear are the unavoidable consequences.

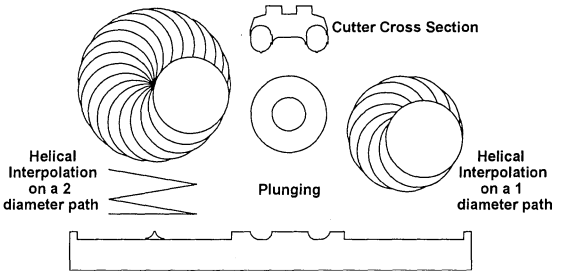

Figure 11. Entering a workpiece with a 2" button cutter utilizing helical interpolation

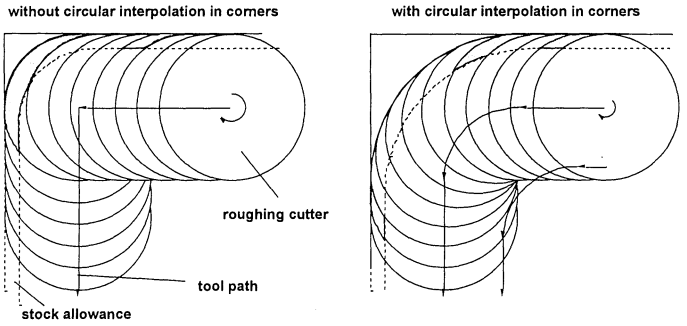

Figure 12. Change in chip thickness when cutting corners in pocketing operations

3.3 Tool Path Optimization for Machining Sculptured Surfaces

With most current CAM systems, the generation of tool paths for milling of sculptured surfaces is mainly based on geometrical considerations. These systems provide little assistance for the selection of optimized milling strategies and parameters. Therefore, an adaptive finish milling strategy was proposed at ERC/NSM and focused on the optimization of tool paths for sculptured surface milling with ball end mills. With the proposed technique, the maximum cutting speed and maximum chip load thickness are maintained within a prescribed narrow range by regulating the spindle speed and feed rate, respectively, depending on the local maximum effective diameter of the cutter. In addition, through discrete representation for the workpiece geometry and cutting edge, the distribution of chip thickness is generated for a specific tool location within the NC program. The chip thickness distribution, which covers several points along the cutting edge and several rotation angles, is then used to determine the extreme cutting conditions. Accordingly, the spindle speed and feed rate are adjusted to generate the desired levels of cutting conditions.

Figure 13 shows a cylindrical surface as an application example of adaptive finish milling. It is clear that the maximum effective diameter changes for each pass, while the total chip thinning factor remains constant. In conventional finish milling, the spindle speed is fixed. Given the variations of maximum effective diameter, the maximum cutting speed changes for each pass. In adaptive finish milling, the maximum cutting speed is maintained within a range by regulating the spindle speed in each pass. Milling time reduction is achieved by adjusting the feed rate according to the spindle speed of each pass and the target maximum chip thickness.

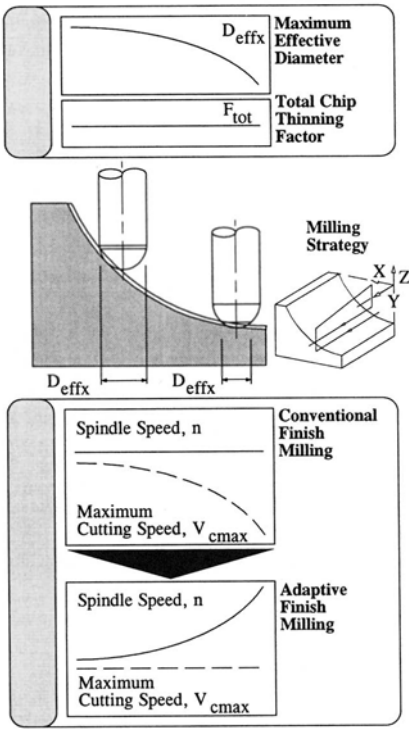

Figure 13. Adaptive finish milling - cylindrical surface [11]

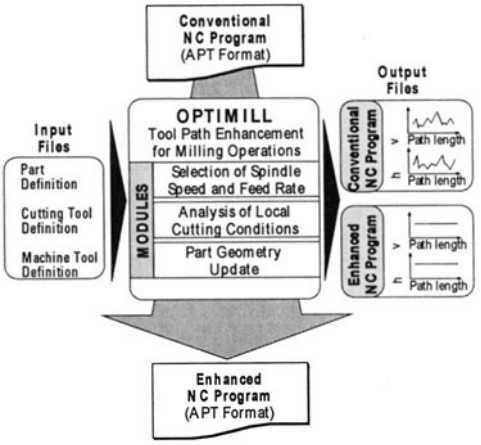

Figure 14. Tool path optimization software 'OPTIMILL'

A prototype computer program (OPTIMILL) was developed to apply the concept of adaptive finish milling, Fig. 14. This software takes an existing NC program in APT format and generates a modified version of the same NC program, with added 'SPINDL' and 'FEDRAT' words to achieve a narrow range of cutting conditions [4]. OPTIMILL performs tool path optimization with three major modules. First, the analysis module provides tool engagement and cutting condition data at a specific tool location. Based on these data, the

optimization module computes the appropriate spindle speed and feed rate. This module also adds 'SPINDL' and 'FEDRAT' words to the original APT file, if necessary. In a final step, the workpiece geometry is updated according to the material removed by the current tool path. The simulation parameters in the input file include resolution specifications for the workpiece representation (mesh) and cutting edge representation (set of nodes). Information about local cutting conditions for both the conventional and optimized NC programs are provided by output files.

Compared to conventional milling techniques, optimized finish milling results in reduction of total milling time and, under certain conditions, longer tool life depending on the tool life characteristics and the target maximum cutting speed [11]. Limited testing of OPTIMILL has shown that, compared to conventional NC programs, reductions in machining time of 20~50% are possible [4].

4. HARD TURNING

The "hard turning" process has been gaining interest as a process that can replace grinding in a certain class of parts. Hard turning equipment is less capital intensive then grinding equipment. In addition, the hard turning process is more then twice as fast as grinding and allows the machining of multiple surfaces in one chucking.

Optimum cutting conditions depend on many parameters. Apart from the workpiece material composition and microstructure, the tool material has an immense influence on surface finish and part accuracy. The high temperatures and specific forces in continuous hard turning require a cutting tool material with high hot hardness and resistance to chipping. Currently only PCBN is suitable for this process. Since the introduction of PCBN as a cutting material, many advances have taken place.

The machine tool determines the repeatability of machining results as well as the attainable form and precision. Because of the small size of the cross section of the chip, there are no special demands on the power of the machine [6]. The main demands are a high static and dynamic stiffness, geometric and kinematic accuracy, and thermal stability.

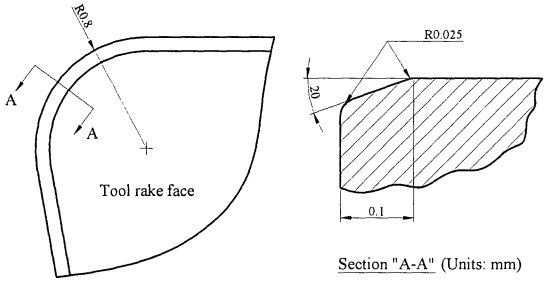

Figure 15. Tool geometry of PCBN inserts

The tool design, in terms of cutting-edge angles, influences chips formation, tool life and repeatability. The cutting tool is subject to extreme mechanical and thermal loads putting high demands on a controlled process. Utilizing the same boundary conditions, the specific components of the cutting forces in HPM double those of soft part machining because of the much higher hardness and strength of the workpiece material [7]. This requires a high level of hardness and binding toughness of the cutting tool. Additionally, most cutting inserts have a chamfer to get a more efficient cutting force vector. Experience indicates that the least amount of tool wear at the tool flank can be reached with chamfers of 20°. A chamfer of 5° has the lowest cratering but results in more chipping [8], which makes the process ineffective.

The main objective of hard turning investigations at the ERC/NSM was to achieve surface finishes within the range of 8~12 μin Ra in hard turning of hardened 1118 steel (60~65 HRC) on a retrofitted lathe. Four different grades of PCBN tool materials were evaluated. They differed by vendor, CBN content, CBN grain size, and binding phase. A secondary aim was to evaluate the "better" PCBN insert type. The supplied PCBN blanks were brazed with silver solder on a corner-notch of a carbide base. The insert type used was CNGA-432T, which incorporated a T-land chamfer 0.1 mm×20° with an additional hone of 0.025 mm and a corner radius of 0.8 mm, Fig. 15.

After the first test batch was run, it became apparent that two of the inserts were performing better than the others. It was decided to eliminate the worst two and concentrate on the most promising insert types. The insert types that were selected for further study were the BZN 8200 from GE SuperAbrasives and the DBC50 from DeBeers. The BZN 8200 was rated at a 2 μin grain size and a 65% CBN content. Unfortunately, GE SuperAbrasives does not share the binding phase make-up. The DeBeers insert was rated at a 1-2 μin grain size and a 50% CBN content. These two inserts were able to withstand the vibrations created by the machine tool for roughly eight bars for BZN8200 and seven bars for DBC50. BZN8200 resulted in an average machined surface roughness of 8 μin while DBC50 provided an average surface roughness of 9 μin.

Hard Turning work at ERC/NSM has just started recently. So far, we have employed the hard turning process to measure flow stress under machining conditions in one project. The other project, as discussed above, had the objective of investigating the feasibility of using the hard turning process on an older retrofitted machine in production. In the course of these projects, we have gained experience in hard turning methods, especially the importance of tool edge preparation and the importance of machine tool/work holder/workpiece rigidity.

5. PREDICTION OF PROCESS VARIABLES IN METAL CUTTING USING FEM & ANALYTICAL TECHNIQUES

5.1 Finite Element Modeling of Metal Cutting

At the ERC/NSM, orthogonal cutting simulation is implemented using "DEFORM". An additional module has been developed and incorporated into this code to predict segmented chip formation by deleting the elements that reach a "critical damage value" that causes fracture, [14]. "DEFORM" is able to automatically remesh the objects and generate a very dense mesh near the tool tip so that it can handle large gradients of strain, strain-rate and temperature. Moreover, the capabilities of automatic remeshing make it possible to study tools with chamfered and rounded edges. Although the assumed input data for material properties and friction were approximated, it was able to simulate various chip shapes with relatively little effort.

a) **Continuous chip formation** and the effects of rake angle, cutting speed, and uncut chip thickness upon chip flow were studied [13]. Continuous chip flow has been also used for orthogonal cutting simulations, using various rake face geometries for cutting speeds up to 1100 m/min, Figure 16 [19]. The validity of the FEA model for orthogonal cutting was tested by comparing the simulation results with experimental data from [18]. In addition, FE simulations were performed to estimate flank wear using wear models, given in the literature [16]. This preliminary investigation demonstrated that with reliable input data on material properties and friction, it is possible to estimate chip flow and cutting forces.

b) **Chip formation in slot milling.** The simulation model has been applied to slot milling with straight cutting edges. The two movements of a milling cutter, linear and rotational movement, have been superimposed which results in variable chip thickness, also referred to as chip thinning. In this case plane strain behavior is assumed and, therefore, 2D simulations give a reasonable representations of the process [29].

c) Segmented chip flow has been investigated in cutting applications with the methodology developed for shearing in blanking simulations [32, 14]. Figure 17 illustrates the effect of rake angle, rake face geometry, and cutting speed upon segmented chip formation. While this work is still very preliminary, it seems to have considerable potential for predicting chip flow that represents "real conditions".

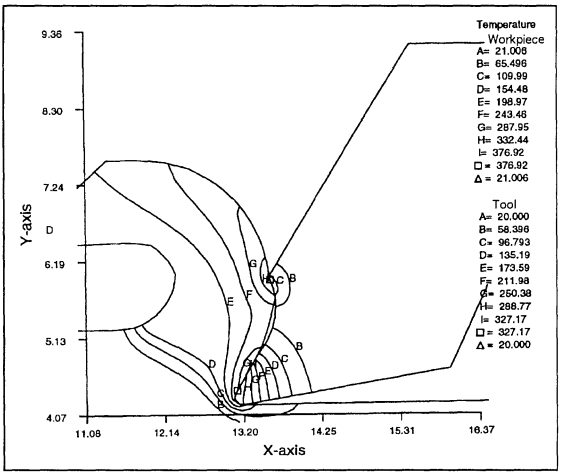

Figure 16. Simulation of orthogonal cutting in AISI 1045 steel with grooved tool (HSS). Temperature contours in tool and workpiece (V_c=250 mm/s, rake angle=30°, uncut chip thickness=1 mm, tool tip radius=0.1 mm, groove radius=2 mm) [19]

5.2 Analytical Modeling of Metal Cutting

A predictive machining theory was developed by Oxley [26]. The theory can calculate forces, temperatures, average stresses, strains, and strain rates from basic material properties of the workpiece (flow stress data and thermal properties), tool geometry and cutting conditions. The basis of the theory is to analyze, in terms of the shear angle ϕ, shown in Figure 18, the stress distributions along the shear plane AB and the tool-chip interface. The value of ϕ is selected such that the resultant forces transmitted by AB and the interface are in equilibrium [27]. Once the value of ϕ is determined, the uncut chip thickness t_2 and the various components of forces can be determined. For orthogonal cutting, the values of the cut chip thickness and the values of forces, predicted by the theory, were found to be in good agreement with experimental results [27].

Oxley's machining theory has been used to:

a) predict cutting forces in oblique turning [22],
b) estimate cutting forces in turning using oblique sharp nose tools [17],
c) predict chip flow and cutting forces in turning using non-oblique nose radius tools [34],
d) estimate temperatures and tool wear rate in orthogonal turning [24],
e) predict cutting forces in face milling using non-oblique nose radius tool [35],
f) obtain chip flow direction and cutting forces in oblique turning with nose radius tools [12].
g) At the ERC/NSM, Oxley's approach has been used to develop a computer program called "OXCUT". This program was designed to compute cutting forces, average values of temperature, effective stress, strain and strain rate in the primary shear zone and secondary shear zone (at the tool-chip interface) for orthogonal cutting, as well as for the extended applications such as ball end milling and face milling using oblique nose radius tools.

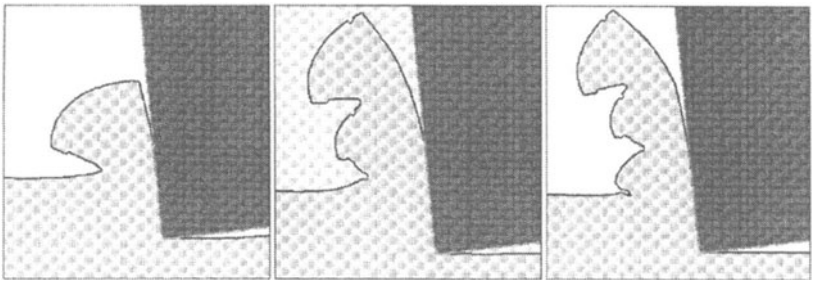

Figure 17. Simulation of segmented chip formation in cutting AISI 1045 steel with HSS tool, (V_c=200 m/min, rake angle=-6°, uncut chip thickness = 0.5 mm) [14].

6. DETEMINATION OF MATERIAL FLOW STRESS UNDER MACHINING CONDITIONS

For practical cutting speeds, the average strain rate values lies within the vicinity of 10^4-10^5 s^{-1}. Many researchers have used high speed compression tests [28] and Hopkinson's impact compression tests [21, 23 & 33] to determine flow stress data for workpiece materials. Due to the difficulty of performing those high speed tests, the flow stress data were obtained at limited and relatively low values of strain rates usually not higher than 2,000 s^{-1}, whereas, the strain rate values encountered in practical machining operations are within the vicinity of 10^4-10^5 s^{-1}.

At the ERC/NSM, the strategy is to analyze the mechanics of metal cutting by using flow stress data determined under realistic cutting conditions. For this purpose, it was attempted to utilize orthogonal cutting tests to estimate flow stress data and friction characteristics at the contact interface.

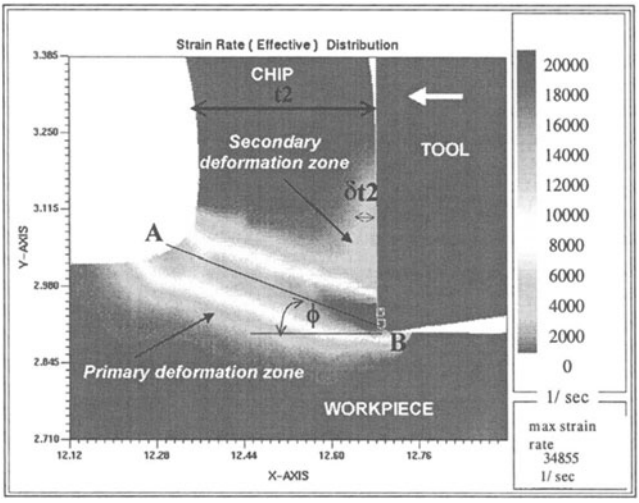

Figure 18. Picture from FEM simulation showing the parameters of Oxley's approach

6.1 Using FEM in Conjunction with Orthogonal Turning Experiments

A methodology was developed to determine simultaneously the flow stress of the workpiece material at high deformation rates, temperatures encountered in the cutting zone,

and friction at the chip-tool interface [29]. This methodology uses the cutting and thrust force data measured from high speed orthogonal cutting experiments in order to calibrate an FEM simulated process model. In the orthogonal cutting process simulations, by using criteria from the cutting conditions (cutting velocity and uncut chip thickness), boundaries of the primary deformation zone (Fig. 18) are identified and the average strain rates and temperatures are computed. Flow stress of the workpiece material at computed average strain rates and temperatures is determined in an iterative scheme until the prediction error for cutting force becomes less than 10%.

In addition, the average strain rates and temperatures are computed at the chip-tool interface and the average shear friction is estimated. The unknown friction coefficients are determined in another iterative scheme until the prediction error for thrust force becomes less than 10%. Therefore, the unknown parameters in the friction model and the flow stress data are estimated simultaneously. This methodology was applied to obtain flow stress for P20 mold steel (at hardness of 30 HRC) and friction data in machining with uncoated tungsten carbide (WC) cutting tool. The experimental cutting conditions of 200-550 m/min cutting speed (V_c), and 0.025-0.100 mm/rev feed rate (V_f) were used.

This methodology uses FEM simulations in conjunction with orthogonal turning experiments. It requires many FEM simulations and iterations, which take considerable time. Therefore, a simpler procedure, using OXCUT, has been developed to obtain the flow stress data.

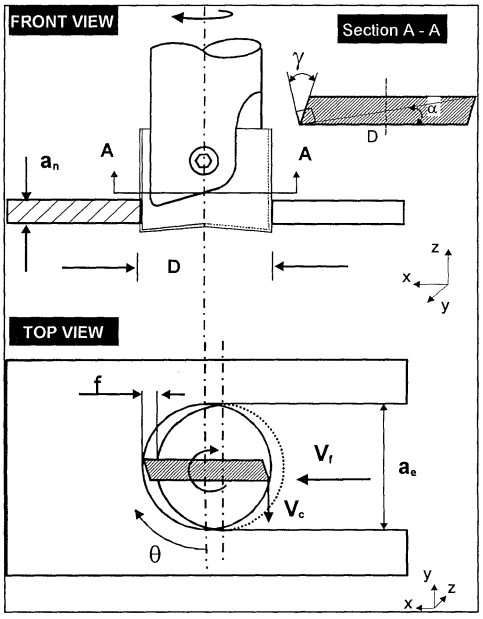

Figure 19. Schematic diagram showing the 2-D orthogonal slot milling

6.2 Using OXCUT in Conjunction with orthogonal Slot Milling Experiments

In this technique cutting and thrust forces are obtained from orthogonal slot milling experiments, Figure 19. These data are compared with those predicted by OXCUT using an initial guess of a flow stress equation. The parameters of the flow stress equation are "tuned" until the forces predicted from OXCUT match those obtained from experiments for all tool rotation angles. The advantage of the suggested technique is that OXCUT only needs calculation time of a few minutes. Moreover, it calculates average strains, strain rates and

temperatures in the primary and secondary deformation zones that match very well with those obtained from FEM.

Furthermore, using orthogonal slot milling tests to obtain flow stress data will help us obtain more states of strains, strain rates and temperatures. This arises from the fact that during each rotation of the cutter, strains, strain rates and temperatures change with the rotation angle due to the variation in depth of cut, Figure 20. Thus, one slot milling experiment in conjunction with one run of OXCUT helps to obtain the flow stress equation that satisfies different conditions of strain, strain rate and temperature. Two or three runs at different orthogonal slot milling conditions will make sure that the obtained flow stress equation is robust enough to be applied within a reasonable range of values of strains, strain rates and temperatures.

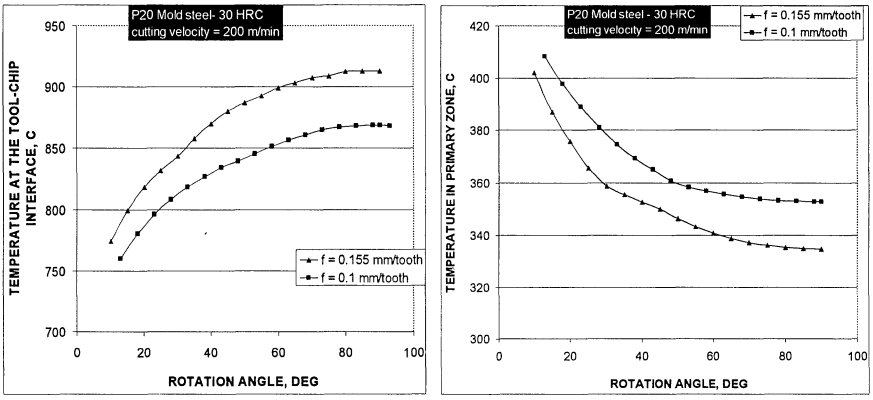

Figure 20. Variation of temperature with rotation angle in the primary zone and at tool-chip interface, predicted from OXCUT in slot milling

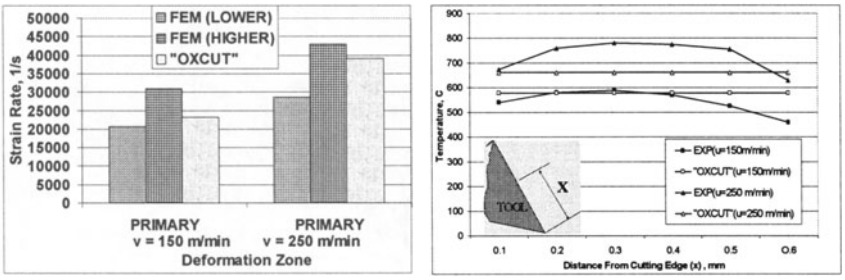

Figure 21. Comparison of OXCUT, FEM and experiment for orthogonal turning of LCFCS [15]

7. APPLICATION OF ANALYTICAL-BASED COMPUTER MODELING (OXCUT) TO PREDICT FORCES, AVERAGE STRESSES AND TEMPERATURES IN METAL CUTTING

7.1 Orthogonal Turning

Figure 21 illustrates a comparison of temperature and effective strain rate predicted from OXCUT, FEM and Childs's orthogonal tests at a cutting speed of 150 and 250 m/min [15]. The workpiece material is low carbon free cutting steel (LCFCS). The tool rake angle, uncut chip thickness and width of cut are 0°, 0.1 mm and 1 mm, respectively. For FEM, the lower

and upper values of the results for the specific zone (primary or secondary) are shown. The contour lines of temperature, effective stress, strain and strain rate obtained from FEM are parallel to the directions of the primary and secondary shear zones [30]. This indicates that the temperature, stress, strain and strain rate do not vary significantly along the shear plane or along the tool-chip interface and are close to the average values predicted from OXCUT.

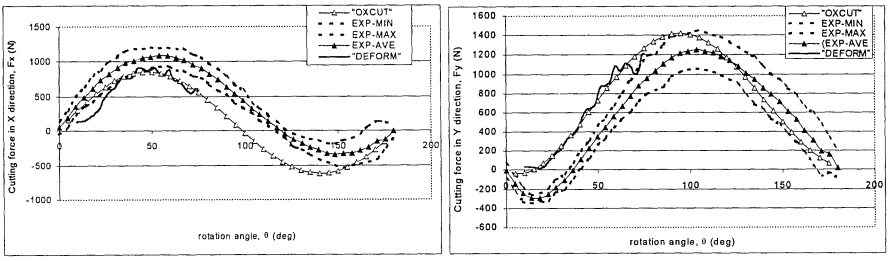

Figure 22. Comparison of OXCUT, DEFORM and experimental results for 2-D slot milling of Ti6Al4V [31]

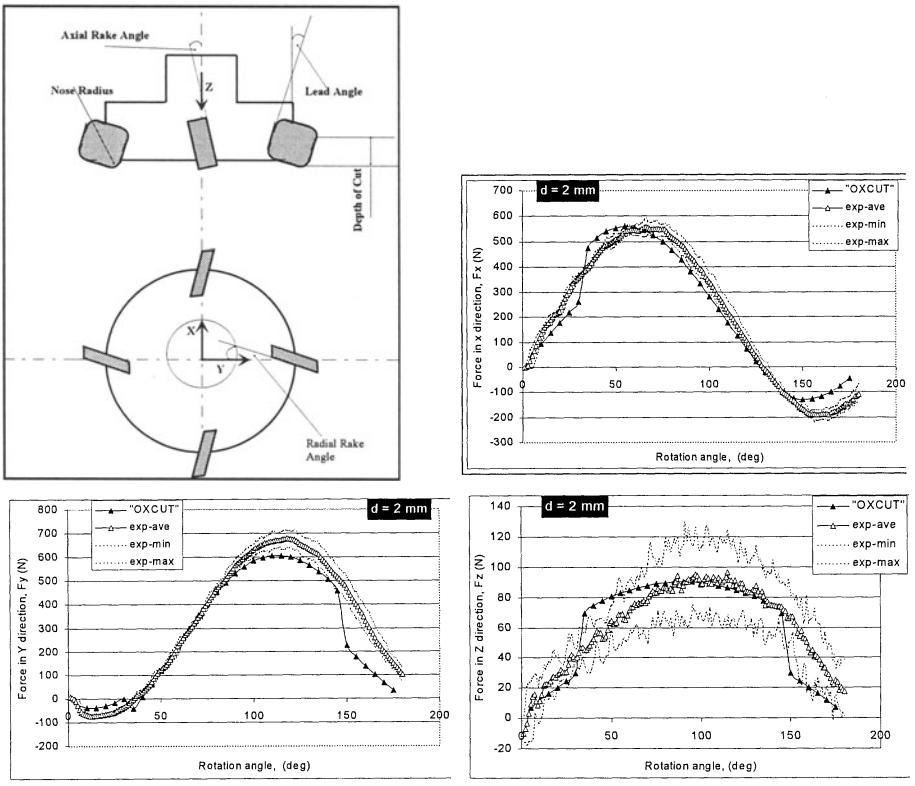

Figure 23. 3-D face milling of P20: experimental and predicted results

7.2 2-D Slot Milling

Figure 22 illustrates a comparison of results obtained from experiment [31], OXCUT and DEFORM of the cutting forces in the X and Y directions vs. tool rotation angle for the slot milling of the titanium alloy Ti6Al4V. Flow stress data and thermal properties of that alloy

are obtained from the literature [21 & 25]. Friction at the tool-workpiece interface was obtained from OXCUT (calculated as part of the solution) and input to DEFORM in addition to the other input data. The tool geometry and cutting conditions of Figure 22 are feed=0.25 mm/rev/tooth, cutting velocity=74.81 m/min, rake angle=0°, clearance angle=7° and width of cut (a_n)=3 mm.

To analyze the slot milling process using OXCUT, the circular tool path is digitized at tool rotation angles in steps of 5° in a manner similar to the work of Young et al. [35]. At each increment, the current depth of cut t_1 at a certain tool rotation angle θ is calculated ($t_1 = f \sin \theta$, f = feed). The cutting and feed forces are calculated using OXCUT for each depth of cut at each angular increment of tool rotation. Then, the cutting and feed forces are transformed into the global X and Y directions to compare with experimental and finite element results.

7.3 3-D Face Milling

Figure 23 shows that three force components predicted by OXCUT are in reasonable agreement with experimental results for 3-D face milling of P20 steel (30 HRC). At each angle of tool rotation, the uncut chip thickness and geometry of equivalent cutting edge are obtained by a similar approach as proposed by Young et al. [35]. The cutting conditions are lead angle = axial rake angle = radial rake angle=0°, depth of cut=2 mm, nose radius=0.8 mm, feed rate=0.1 mm/tooth, and cutting speed=200 m/min.

The work of Young et al. was extended at the ERC/NSM to analyze face milling with inserts of non-zero axial and radial rake angles. This is done by using 3-D vector analysis to calculate the normal rake angle of the insert at each tool rotation angle and considering the axial rake angle as the inclination angle. Then, at each tool rotation angle, the equivalent cutting edge and cutting forces are obtained in a manner similar to the analysis of oblique turning, using nose radius inserts, done by Arsecularante et al. [12].

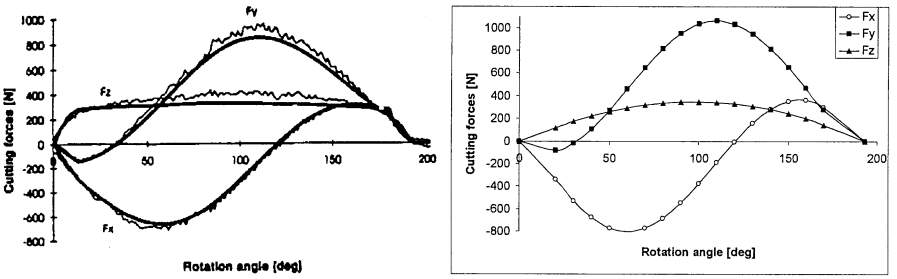

Figure 24. Ball end milling of Ti6Al4V (ball nose radius=9.525 mm, normal rake angle=5°, feed=0.1016 mm/flute, axial depth of cut=3.81 mm, flutes=1, spindle speed=269 rpm, inclination angle=30°).

7.4 Ball End Milling of Ti6Al4V

The ball end mill is divided into slabs in a manner similar to the work of Lee and Altintas [20]. A computer program was written to calculate the oblique parameters (e.g. normal rake angle, inclination angle and depth of cut) associated with each slab. This code was integrated into OXCUT to predict cutting forces, average temperatures and stresses at the tool rake face for each slab. The calculated slab forces were then resolved into the X, Y and Z directions and summed up for all slabs to obtain the resultant cutting forces. In the case of ball end milling of Ti6Al4V, the force components obtained experimentally and analytically in the literature [20] (top) are compared with those predicted by OXCUT (bottom) in Figure 24. Flow stress data and thermal properties were obtained from the literature [21].

8. APPLICATION OF FEM TO ESTIMATE DISTRIBUTIONS OF TEMPERATURE AND STRESSES IN METAL CUTTING

8.1 Orthogonal Turning

DEFORM simulations were performed with the same cutting conditions and workpiece material (LCFCS) as those used by Childs et al [15]. The rake angle and feed rate of tool were 0° and 0.1 mm, respectively. The cutting velocity was 150 m/min. Flow stress and contact friction data at the tool-chip interface were obtained from the literature [15]. Figure 25 shows the predicted temperature distribution in °C for the tool and workpiece. Through FEM simulation, the predicted data of stress, temperature and relative velocity on the tool rake face and flank face may then be applied to estimate volumetric rates of crater wear and flank wear of the tool.

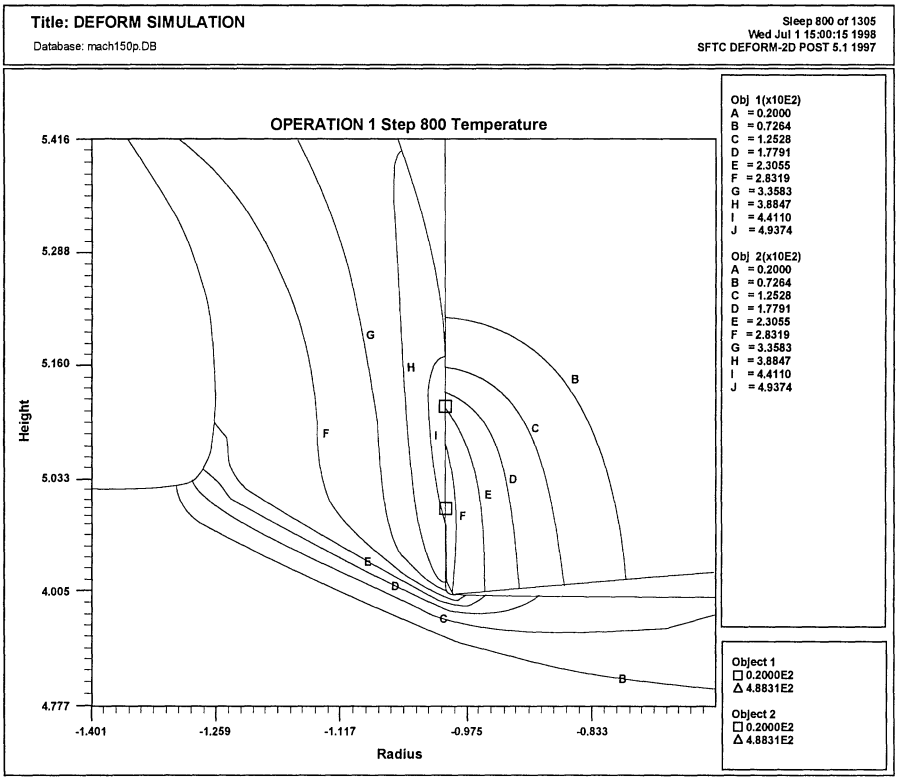

Figure 25. Temperature distribution (°C) predicted from FEM simulation for orthogonal turning of LCFCS (cutting speed=150 m/min, rake angle=0°, depth of cut=0.1 mm.

8.2 2-D Slot Milling

FEM simulation using DEFORM was also used in analyzing the 2-D orthogonal slot milling operation [29]. The workpiece material used was P20 mold steel hardened to 30 HRC. Flow stress and friction data were given in the literature [23]. In this case, the uncut chip thickness changes continuously due to the simultaneous linear translation as the tool rotates. The feed rate and cutting speed were 0.155 mm/tooth and 200 m/min. The rake angle, clearance angle and hone radius of the tool were –11.4°, 17.9°, and 0.012 mm, respectively.

Figure 26 shows the temperature distribution (°C) for the tool and workpiece at a rotation angle of 72°. The cutting forces predicted by FEM simulations were found to be in good agreement with those obtained from experiment [29].

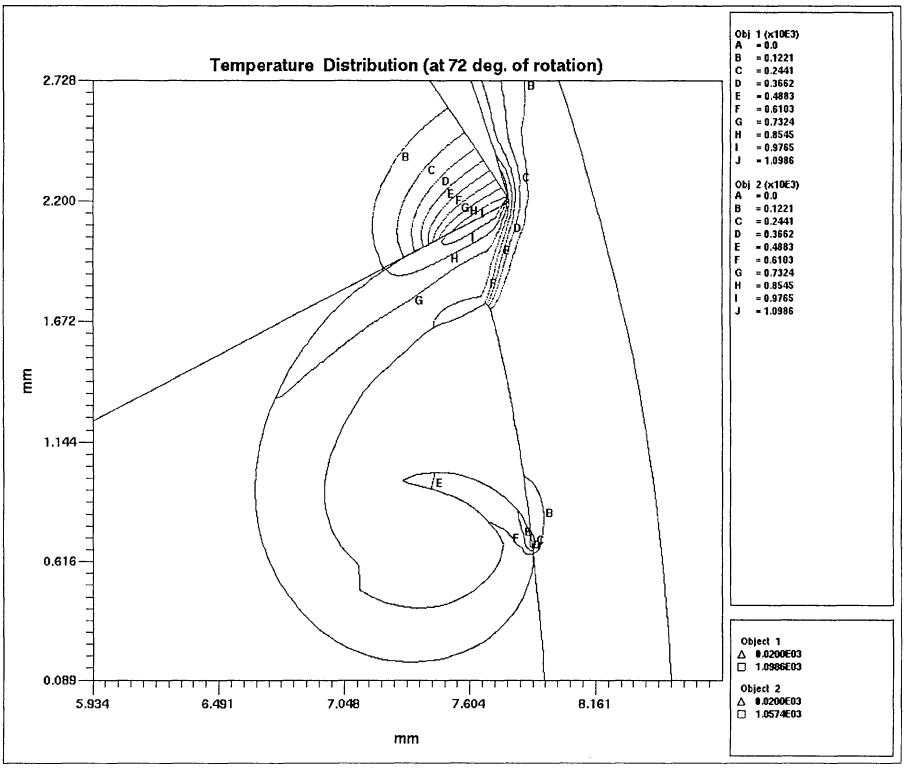

Figure 26. Temperature distribution (°C) predicted from FEM simulation for 2-D slot milling of P20 mold steel at a rotation angle of 72° (hardness =30 HRC, feed rate =0.155 mm/tooth, cutting speed =200/min,)

9. SUMMARY AND CONCLUSIONS

In recent years High Speed Cutting (HSC) technology is increasingly used in machining of dies and molds. The objectives are to reduce lead times while increasing dimensional tolerances and surface integrity. The cost-effective application of HSC requires advances in all components of the HSC system, including: machine tools, spindles and tool holders, controllers, NC programming strategy, tool materials and coatings, reliability and process knowledge.

Similar to other relatively new and leading edge manufacturing technologies, the application of HSC will continue to increase with the knowledge base and the detailed understanding of the process. The high temperatures and stresses, developed in HSC, are greatly influenced by tool insert design (geometry, material and coating). Ongoing research indicates that cutting temperatures and stresses can be predicted with reasonable accuracy, using FEM analysis. These predictions have the potential to allow the a) prediction and control of tool failure (diffusion, wear and chipping), b) optimization of cutting variables to extend tool life and improve surface integrity, and c) design of inserts for specific applications.

In the future, we can expect process simulation will be very helpful to optimize tool design and eliminate premature tool failure, thus contributing to expand the areas of application of HSC technology.

Parallel to FEM applications, it is still useful to utilize analytical-based modeling to predict cutting forces, average contact stresses and temperatures as well as to determine flow stress data from cutting experiments.

REFERENCES

1 Dewes, R. C. and Aspinwall, D. K. (1997). A review of ultra high speed milling of hardened steels, Journal of Materials Processing Technology, 69, 1-17.

2 Schulz, H. and Moriwaki, T. (1992). High-Speed Machining, Annals of the CIRP, 41(2), 637-643.

3 Fallböhmer, P., Altan, T., Tönshoff, H. K. and Nakagawa, T. (1996). Survey of the Die and Mold Manufacturing Industry, Journal of Materials Processing Technology, 59, 158-168.

4 Bergs, T., Rodríguez, C. A., Akgerman, N. and Altan, T. (1996). Tool Path Optimization for Finish Milling of Die and Mold Surfaces – Software Development, Transactions of NAMRI/SME, 24, 81-86.

5 Kaiser, M. (1992). Hartfeinbearbeitung von einsatzgehaertetem Stahl mit PKB Werkzeugen, IDR, 1, 18-24.

6 Bussmann, W. and Stanske, C. (1986). Hartbearbeitung durch die Fertigungsverfahren Drehen und Fraesen, tz fuer Metallverarbeitung, 12.

7 König, W., Goldstein, M. and Iding, M. (1988). Drehen gehaerter Stahlwerkstoffe, Industrie Anzeiger, 14.

8 Stanske, C. (1993). Werkzeuge für die moderne Fertigung, Reihe Kontakt und Studium, Fertigung, 370, 288-316.

9 Abrao, A. M., Aspinwall, D. K. and Wise, M. L. H. (1993). A Review of Polycristalline Cubic Boron Nitride Cutting Tool Developments and Applications, Proceedings of the 13th International Matador Conference, March 31st – April 1st, Manchester.

10 Neises, A. (1995). Einfluß von Aufbau und Eigenschaften hochharter nichtmetallischer Schneidstoffe auf Leistung und Verschleiß im Zerspanprozß mit geometrisch bestimmter Schneide, Fort. Ber. VDI, Reihe 2: Fertigungstechnik Nr.: 332. Düsseldort: VDI Verlag.

11 Gaida, W., Rodríguez, C. A., Altan, T. and Altintas, Y. (1995). Preliminary Experiments for Adaptive Finish Milling of Die and Mold Surfaces with Ball-nose End Mills, Transactions of NAMRI/SME, 193-198.

12 Arsecularante, J. A., Mathew, P., and Oxley, P. L. B. (1995). Prediction of Chip Flow Direction and Cutting Forces in Oblique Machining with Nose Radius Tools, Proc. Inst. Mech. Engrs, 209, 305-315.

13 Ceretti, E. , Fallböhmer, P. , Wu, W.T., Altan, T. (1996). Application of 2D FEM to Chip Formation in Orthogonal Cutting, Journal of Materials Processing Technology, 59, 169-181.

14 Ceretti, E., Taupin, E., Altan, T. (1997). Simulation of Metal Flow and Fracture-Applications in Orthogonal Cutting, Blanking, and Cold Extrusion, Annals of the CIRP, 46, Jan./1997.

15 Childs, T.H., Dirikolu, M.H., Sammons, M.D.S., Maekawa, K., and Kitagawa, T. (1997). Experiments on and Finite Element Modeling of Turning Free-Cutting Steels at Cutting Speeds up to 250 m/min, Procs. of 1st French and German Conference. On High Speed, Mar., 325-331.

16 Felder, E., and Montagut, J.L. (1980). Friction and Wear During the Hot Forging of Steels, Tribology International, 61-68.

17 Hu, R. S., Mathew, P., Oxley, P. L. B., and Young, H. T. (1986). Allowing for End Cutting Edge Effects in Predicting Forces in Bar Turning with Oblique Machining Conditions, Proc. Inst. Mech. Eng., 200, C2, 89-99.

18 Iwata, K., Osakada, K., Terasaka, Y. (1984). Process Modeling of Orthogonal Cutting by the Rigid-Plastic Finite Element Method, Journal of Engineering for Industry (ASME), 106, 132-138.

19 Kumar, S., Fallböhmer, P., Altan, T. (1996). Finite Element Simulation of Metal Cutting Processes: Determination of Material Properties And Effects of Tool Geometry On Chip Flow, Report No. D-96-17, ERC/NSM, The Ohio State University.

20 Lee, P. and Altintas, Y. (1996). Prediction of Ball-End Milling Forces From Orthogonal Cutting Data, Int. J. Mach. Tool Manufact., 36, 9, 1059-1072.

21 Lee, W. and Lin, C. (1998). High-Temperature Deformation Behavior of Ti6Al4V Alloy Evaluated by High Strain-Rate Compression Tests, Journal of Materials Processing Technology, 75, 127-136.

22 Lin, G. C. I., Mathew, P., Oxley, P. L. B., and Watson, A. R. (1982). Predicting Cutting Forces for Oblique Machining Conditions, Proc. Inst. Mech. Eng. 196, 141-148.
23 Maekawa, K., Shirakashi, T., and Usui, E. (1983). Flow Stress of Low Carbon Steel at High Temperature and Strain Rate (Part 2), Bull. Japan Soc. of Prec. Engr., 17, 3, 167-172.
24 Mathew, P. (1989). Use of Predicted Cutting Temperatures in Determining Tool Performance, Int. J. Mach. Tools Manufact., 29, 4, 481-497.
25 Obikawa, T. and Usui, E. (1996). Computational Machining of Titanium Alloy – Finite Element Modeling and a Few Results, Transactions of the ASME, 118, 208-215.
26 Oxley, P.L.B. (1966). Introducing Strain-rate Dependent Work Material Properties into the Analysis of Orthogonal Cutting, Annals of the CIRP, 13, 127-138.
27 Oxley, P.L.B. (1989). Mechanics of Machining - An Analytical Approach to Assessing Machinability, Halsted Press: a division of John Wiley & Sons Limited, New York.
28 Oyane, M., Takashima, F., Osakada, K., and Tanaka, H. (1967). The Behavior of Some Steels Under Dynamic Compression, 10th Japan Congress on Testing Materials, 72-76.
29 Özel, T. (1998). Investigation of High Speed Flat End Milling Process, Ph.D. Dissertation, The Ohio State University.
30 Shatla, M. and Altan, T. (1998). Use of Analytical-Based Computer Modeling to Analyze 2-D and 3-D Turning and Face Milling Operations, Report No. HPM/ERC/NSM-98-R-28, ERC/NSM, The Ohio State University.
31 Sterr, M. (1998). Private Communication with Fraunhofer Institute, Boston.
32 Taupin, E., Breitling, J., Altan, T. (1996). Material Fracture and Burr Formation in Blanking – Results of FEM Simulations and Comparison with Experiments, Journal of Materials Processing Technology, 59, 66-78.
33 Usui, E. and Shirakashi, T. (1982). Mechanics of Machining -from Descriptive to Predictive Theory. In On the Art of Cutting Metals-75 years Later, ASME Publication PED 7, 13-35.
34 Young, H. T., Mathew, P., and Oxley, P. L. B. (1987). Allowing for Nose Radius Effects in Predicting the Chip Flow Direction and Cutting Forces in Bar Turning, Proc. Inst. Mech. Engrs., 201, C3, 213-226.
35 Young, H. T., Mathew, P., and Oxley, P. L. B. (1994). Predicting Cutting Forces in Face Milling, Int. J. Mach. Tools Manufact., 34, 6, 771-783.